Angular Motions of a Rocket due to Thrust with a Ramp Input

TADEUSZ PAPIS*
McDonnell Douglas Corporation, Newport Beach, Calif.

Customarily treated as a step input, a body-fixed moment due to thrust is more closely represented by a ramp input. Prompted by concern about this discrepancy, the analysis presented here yielded detailed yet completely general results in a parameterized form. These show that when a body fixed moment is applied as a ramp input rather than as a step input 1) the cross-spin and hence the coning angle are always decreased, 2) the average attitude error may be increased or decreased, and 3) under certain conditions both the coning angle and displacement of the center of motion may be zero, individually or simultaneously. The most important parameter governing the outcome is the number of spin revolutions performed by the body during thrust rise, with inertia ratio being another factor of consequence. Graphs permitting rapid reconstruction of motions for different inputs and inertia ratios are presented. Results of the analysis are shown to have wide applicability to interpretation of angular motion patterns and are used to explain meaningfully thrusting phase and burn-out phenomena.

Nomenclature†

A,C	=	pitch and roll inertias, respectively
a	=	amplitude of precession when $t \leq \Delta t$
a'	=	amplitude of precession when $t \geq \Delta t$
a^*	=	amplitude of precession in the case of a step input ($\Delta t = 0$)
b	=	amplitude of nutations at $t \leq \Delta t$
b'	=	amplitude of nutations at $t \geq \Delta t$
c	=	center of motion at $t \leq \Delta t$
c'	=	center of precession at $t \geq \Delta t$
c^*	=	center of precession when $\Delta t = 0$ (step input)
M	=	constant body-fixed moment; $\dot{M} = M/\Delta t$
n	=	spin velocity, constant
N,N_λ	=	$n \cdot \Delta t/2\pi$, and $\lambda \cdot \Delta t/2\pi$, respectively
R	=	A/C, inertia ratio
t	=	time from ignition
Δt	=	time of thrust, or moment M, rise
t'	=	$t - \Delta t$
λ	=	$(C - A)n/A$
β	=	$M/(C - A)n^2$ (equivalent asymmetry); $\dot{\beta} = \beta/\Delta t$
θ	=	attitude angle in inertial axes; $\dot{\theta} = \partial\theta/\partial t$
ω	=	angular velocity in body-fixed axes
X,Y,Z	=	inertial axes system
1,2,3	=	body-fixed principal axes system
x,y,z	=	body-fixed axes system inclined to 1,2,3 at an angle β

Introduction

THE effect of a body-fixed external moment upon angular motions of a spin-stabilized rocket in vacuum has been investigated at length by Jarmolow,[1] Suddath,[2] and Buglia et al.[3] Although their analyses differ widely in scope and objectives, they all apply the external moment as a step input. A literature survey by this writer indicates this to be a standard procedure. Implicit it is in the assumption of an instantaneous thrust rise. In reality, thrust rise is not instantaneous but extends over a finite time interval of about 0.2–1 sec. Also, there is a common tendency to discuss the results in terms of mathematical parameters, which often do not clearly or properly reflect some important physical phenomena, due to simplifying assumptions made in the process of formulating or solving the mathematical problem. Discussions are usually supplemented by illustrations of some arbitrarily selected "typical cases" of angular motion patterns, obtained with the use of advanced computing machinery. These, although useful, are quite likely to mislead, because identical patterns can be obtained under totally different conditions.

The present analysis arose out of concern about the effect of the discrepancy between actual and assumed conditions upon angular motions of a rocket in general and upon the average attitude error during burning in particular, the latter being of special importance in orbital analyses. It was further prompted by the need for analytical results that would be readily applicable to an unambigous and relatively straightforward interpretation of flight test data related to angular motions of a rocket in space. To focus attention on the main issues of consequence, a simple analytical model with constant mass properties and no jet damping will be considered. The results obtained on the basis of that model will be subjected to a detailed discussion in physical terms, which will extend their practical utility well beyond the original problem statement. In particular, these results will be shown to be applicable to a meaningful interpretation of thrusting phase phenomena with variable moment, variable inertia, and jet damping taken into account.

Problem Statement

Consider a slender body of revolution spinning with a uniform angular velocity n about the axis of symmetry 3 of the body principal axes system 1,2,3 acted upon by a body-fixed moment increasing linearly from zero at $t = 0$ to some final value M at $t = \Delta t$ and thereafter remaining constant. At $t = 0$ rotating axes 1,2,3 are coincident with the inertial coordinates X,Y,Z and the transverse angular velocity is zero. We shall investigate the ensuing angular motions, and the question of particular interest will be the final attitude displacement, measured by an angle between the body axis 3 and the space-fixed axis Z.

Motions in Body Principal Axes

To simplify notation in the analysis which follows, unless otherwise indicated, M and β stand for values at $t = \Delta t$;

Received April 9, 1969; revision received October 31, 1969. The author gratefully acknowledges his indebtedness to J. L. Junkins of the McDonnell Douglas Astronautics Company, who suggested, formulated and executed the numerical computational scheme to obtain results presented in Figs. 8 and 9, and to W. E. Carr, of the McDonnell Douglas Astronautics Company, without whose support this paper would not have been published.

* Senior Engineering Specialist, Feher Cycle Project, Astropower Laboratory, Western Division. Member AIAA.

† Second Euler Angles scheme and notation are employed.

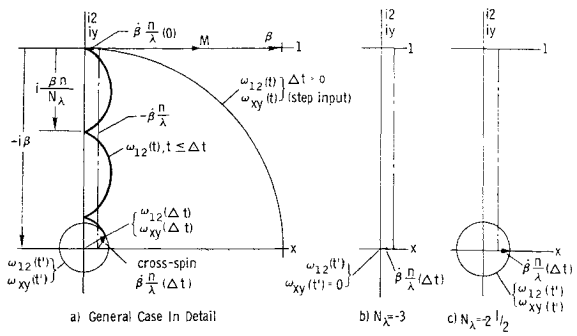

Fig. 1 Transverse angular velocities in body axes under ramp input of M, $A/C = 10$.

but we shall still write simply $\dot{M}$ and $\dot{\beta}$ for the slopes of $M(t)$ and $\beta(t)$ at $t \leq \Delta t$. Also, the principal body-fixed axes system is chosen so that the body-fixed moment vector lies along the axis 1. Thus Euler equations in the axes 1,2 can be written in a complex form as follows[4]:

$$\dot{\omega}_{12} - i\lambda\omega_{12} = \dot{M}t/A, \quad 0 \leq t \leq \Delta t \tag{1}$$

and

$$\dot{\omega}_{12} - i\lambda\omega_{12} = M/A, \quad t \geq \Delta t \tag{2}$$

where

$$\lambda = (C - A)n/A \quad \text{and} \quad \dot{M} = M/\Delta t$$

Solving (1) and (2),

$$\omega_{12}(t) = (\dot{M}/A\lambda^2)(1 - e^{i\lambda t} + i\lambda t), \quad t \leq \Delta t \tag{3}$$

and

$$\omega_{12}(t) = \omega_{12}(\Delta t)e^{i\lambda(t-\Delta t)} + i(M/A\lambda)\{1 + e^{i\lambda(t-\Delta t)}\}, \quad t \geq \Delta t \tag{4}$$

From (3),

$$\omega_{12}(\Delta t) = (M/A\lambda)\{i + (1/\lambda\Delta t)(1 - e^{i\lambda\Delta t})\} \tag{5}$$

Putting (5) into (4) and denoting $(t - \Delta t)$ by t', we obtain

$$\omega_{12}(t') = (M/A\lambda)\{i + (1/\lambda\Delta t)(1 - e^{i\lambda\Delta t})\cdot e^{i\lambda t'}\} \tag{6}$$

Now note that

$$\Delta t = 2\pi N/n = 2\pi N_\lambda/\lambda \tag{7}$$

where N is the number of revolutions executed by the body during the time interval from $t = 0$ to $t = \Delta t$, and N_λ is the number of revolutions performed during the same time by the rotating vector $-M/A\lambda^2\cdot\Delta t$ with respect to the body-fixed axes 1,2. Expressing Δt in terms of N_λ and λ, we obtain

$$\omega_{12}(t) = M/2\pi N_\lambda\cdot(1/A\lambda)(1 - e^{i\lambda t} + i\lambda t) \tag{8}$$

$$\omega_{12}(\Delta t) = (M/A\lambda)\{i + (1/2\pi N_\lambda)(1 - e^{i2\pi N_\lambda})\} \tag{9}$$

$$\omega_{12}(t') = (M/A\lambda)\{i + (1/2\pi N_\lambda)(1 - e^{i2\pi N_\lambda})e^{i\lambda t'}\} \tag{10}$$

If N_λ is an integer, then $e^{i2\pi N_\lambda} = 1$ and at $t \geq \Delta t$

$$\omega_{12}(t') = iM/A\lambda = \omega_{12}(\Delta t) = \text{const}$$

i.e., there will be no wobble.

If moment is applied gradually, such that N_λ is large, then $\omega_{12}(t') = \omega_{12}(\Delta t) = iM/A\lambda$ (a constant), i.e., there will be practically no wobble.

In (10) as $N_\lambda \to 0$, $t' \to t$ and $(1/2\pi N_\lambda)(1 - e^{i2\pi N_\lambda}) \to -i$. Therefore

$$\omega_{12}(t')_{\Delta t \to 0} = \omega_{12}(t) = i(M/A\lambda)(1 - e^{i\lambda t}) \tag{11}$$

which is a well-known result for a step input constant moment.[4]

It follows from elementary considerations that application of a small body-fixed moment M to a perfectly symmetric body of revolution is dynamically equivalent to introduction of a small dynamic unbalance (i.e., product of inertia), or to tilting the principal axis with respect to the axis of symmetry by a small angle β. The product of inertia which can produce moment vector M is given by $-iM/n^2$; hence, and from elementary derivations of the principal axes,[5] it can be readily shown that the angle β measured in the counterclockwise direction from the axis of symmetry is given by

$$\beta = -M/(C - A)n^2 = -M/A\lambda n \tag{12}$$

where β is expressed as a vector, i.e., $\beta = i\hat{\beta}$. Thus the orthogonal system x,y,z originally coincident with the 1,2,3 system but later (upon application of the moment) rotated about the x axis through an angle β can be looked upon as the principal axes of the equivalent moment free system.

Making use of (12), Eqs. (8) and (10) can be rewritten in the following very useful forms:

$$\omega_{12} = -i\beta(t)n - \dot{\beta}(n/\lambda)(1 - e^{i\lambda t}) \tag{13}$$

where $\beta(t) = \dot{\beta}t$, and

$$\omega_{12}(t') = -i\beta n - \dot{\beta}\,(n/\lambda)(1 - e^{i\lambda\cdot\Delta t})e^{i\lambda t'} \tag{14}$$

where β is the final equivalent misalignment angle at $t \geq \Delta t$.

Detailed graphical interpretation of motions in body axes is provided in Fig. 1, where (1b) and (1c), which depict special cases $N_\lambda = -3$ and $N_\lambda = -2\frac{1}{2}$ are restricted to motions at $t \geq \Delta t$ in the interest of clarity. While the figures are meant to be self-explanatory, the following observations may be in order:

1) When the applied moment is constant, the z axis of the equivalent moment-free system x,y,z constitutes the spin axis of the body.

2) If a constant moment is applied as a step input, the instantaneous tilt of the spin axis through an angle β is accompanied by instant formation of the cross-spin velocity vector $i\beta n$ rotating about the z axis at a constant rate λ. Thus $\omega_{xy} = i\beta ne^{i\lambda t}$. Note that the vector angle β lies always along the intersection of the planes of x-y and 1-2. Upon translation of the transverse rate ω_{xy} to the axes 1-2, we obtain $\omega_{12} = -i\beta n(1 - e^{i\lambda t})$.

3) When the applied moment increases linearly from the initial value of zero, then for a given body the magnitude of the "wobble" depends upon $\dot{\beta}$ alone, it being given by $\dot{\beta}n/\lambda$. This cross spin velocity vector rotates about the body spin axis displaced by an angle $-\dot{\beta}/\lambda$ from the z axis which tilts from the axis of symmetry at the rate $\dot{\beta}$. The nonrotating transverse velocity component in the 1-2 axis, viz., $-\dot{\beta}n/\lambda$, does not constitute a "wobble"; its presence is solely the result of resolution of the spin velocity n in the system 1,2,3.

4) Upon moment $M(t)$ reaching its steady state value M, the z axis becomes the spin axis, and the transverse velocity component $\omega_{xy}(\Delta t) = -\beta n/\lambda(1 - e^{i\lambda\cdot\Delta t}) = -\beta n/2\pi N_\lambda(1 - e^{i2\pi N_\lambda})$ becomes the cross-spin velocity vector rotating about z.

5) The change in the magnitude of the cross-spin velocity vector, associated with the transfer of its origin to z axis upon moment M achieving its steady state value is contingent upon the change in the slope $\dot{M}$ (or $\dot{\beta}$) taking place instantaneously. Had the moment M tapered off gradually, the cross-spin $\beta n/\lambda$ would have been transferred to the z axis without any change in its magnitude.

6) As $\Delta t \to 0$, $\beta \to \infty$, but $\omega_{xy_{\max}} = -i\beta n$, which is the result for the step input case.

Motion in Inertial Coordinates

When attitude displacement θ is small, $\theta_{XY} = \omega_{12}\cdot e^{int}$ (Ref. 4). Therefore, upon transformation to inertial coordinates, Eqs. (13) and (14) become, respectively,

$$\dot{\theta}_{XY}(t) = -\dot{\beta}(itn + n/\lambda)e^{int} + (\dot{\beta}n/\lambda)e^{i(n+\lambda)t} \tag{15}$$

and

$$\dot{\theta}_{XY}(t') = -i\beta n \cdot e^{int'} - (\dot{\beta}n/\lambda)(1 - e^{i\lambda\cdot\Delta t}) \cdot e^{i(n+\lambda)t'} \quad (16)$$

Integrating (15) subject to $\theta_{XY}(0) = 0$, we obtain an expression for angular motion in inertial space executed by the axis of symmetry of the body, when applied moment increases linearly:

$$\theta_{XY}(t) = i\frac{\dot{\beta}}{n}\left\{\frac{\lambda}{\lambda + n} + \left(\frac{n - \lambda}{\lambda} + int\right)\cdot e^{int} - \frac{n}{\lambda}\cdot\frac{n}{n + \lambda}\cdot e^{i(n+\lambda)t}\right\} \quad (17)$$

where $\dot{\beta} = -(M/A\lambda n)\cdot(1/2\pi N)$. In geometrical interpretation of motion the radius vector $-(\dot{\beta}/\lambda)\cdot[n/(n + \lambda)]$ rotating with an angular velocity $n + \lambda$ is the constant coning angle of precessional motion about a fixed point in space $c = i(\beta/n)\cdot[\lambda/(\lambda + n)]$; the amplitude of nutations consists of a time-varying angle $-\beta t$ between the axes z and 3, and a constant term $i(\beta/\lambda)\cdot[(n - \lambda)/n]$. In a strict sense of dynamics, the precessional motion takes place about the total angular momentum vector rotating with velocity n in a circle of radius $i(\beta/\lambda)\cdot[(n - \lambda)/n]$ about the point c. However, in either interpretation the point c is the center of motion, fixed in space.

At $t = \Delta t$ the moment attains its constant value and

$$\theta_{XY}(\Delta t) = i\frac{\beta}{\Delta t n}\left\{\frac{\lambda}{\lambda + n} - \frac{n}{\lambda}\cdot\frac{n}{n + \lambda}\cdot e^{i(n+\lambda)\cdot\Delta t} + \frac{n - \lambda}{\lambda}e^{in\cdot\Delta t}\right\} - \beta\cdot e^{in\cdot\Delta t} \quad (18)$$

where

$$n\cdot\Delta t = 2\pi N \quad \text{and} \quad \beta = -M/A\lambda n$$

To obtain steady-state motion, we integrate Eq. (16) and determine the constant of integration from the condition that at $t' = 0$, $t = \Delta t$ and $\theta_{XY} = \theta_{XY}(\Delta t)$ as given by (18). After some rearrangement, the result is

$$\theta_{XY}(t') = c' + a'e^{i(n+\lambda)t'} + b'e^{int'} \quad (19)$$

where

$$c' = -i(\dot{\beta}/\lambda)\cdot[n/(n + \lambda)](1 - \lambda^2/n^2 - e^{i\lambda\cdot\Delta t})(1 - e^{in\cdot\Delta t}) \quad (19a)$$

is the center of precession,

$$a' = i(\dot{\beta}/\lambda)\cdot[n/(n + \lambda)](1 - e^{i\lambda\cdot\Delta t}) \quad (19b)$$

is the radius vector of precession at $t = \Delta t$, and

$$b' = -\beta\cdot e^{in\cdot\Delta t} \quad (19c)$$

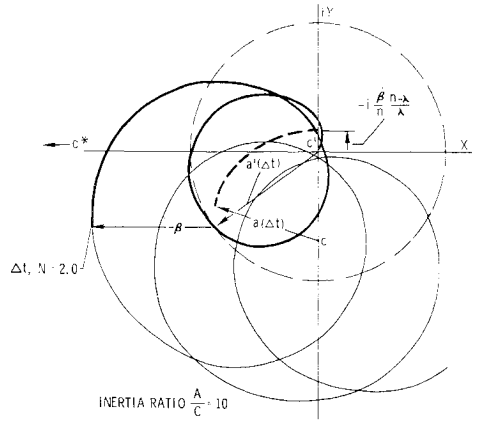

Fig. 2 Body attitude under ramp input; $c' = 0$.

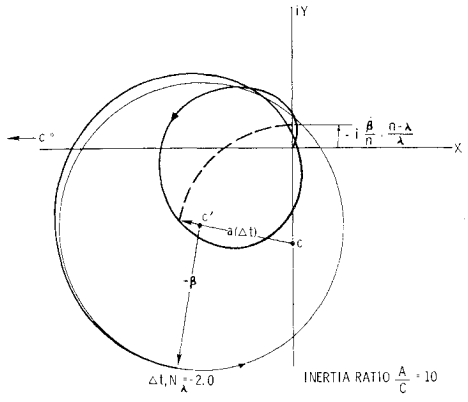

Fig. 3 Body attitude under ramp input; $a' = 0$.

is the radius vector of nutations at $t = \Delta t$, now constant in magnitude.

In (19a) and (19b) taking the limit $\Delta t \to 0$, we obtain

$$c'_{\Delta t\to 0} = c_{\Delta t\to 0} = \beta\lambda/(n + \lambda) = c^*$$

$$a'_{\Delta t\to 0} = a_{\Delta t\to 0} = \beta n/(n + \lambda) = a^*$$

Therefore,

$$\theta_{XY}(t')_{\Delta t\to 0} = \theta_{XY}(t)_{\Delta t\to 0} = \beta\{\lambda/(n + \lambda) + [n/(n + \lambda)]e^{i(n+\lambda)t} - e^{int}\} \quad (20)$$

which is a well-known form for a near-symmetric body of revolution, or for a perfectly symmetric body under constant body-fixed moment with a step input if β is replaced by $-M/A\lambda n$.

Further analysis of angular motions at $t \geq \Delta t$ can be conveniently carried out in terms of c'/c^* and a/a^* ratios. Replacing $n\cdot\Delta t$ and $\lambda\cdot\Delta t$ by $2\pi N$ and $2\pi N_\lambda$, respectively

$$c'/c^* = -(i/2\pi N_\lambda)\cdot(n/\lambda)(1 - \lambda^2/n^2 - e^{i2\pi N_\lambda})(1 - e^{i2\pi N}) \quad (21)$$

and

$$a'/a^* = (i/2\pi N_\lambda)(1 - e^{i2\pi N_\lambda}) \quad (22)$$

Note that for a given body both ratios are functions of N only. Several other observations can be made:

1) If N is an integer, then $c' = 0$, i.e., the mean attitude displacement at $t \geq \Delta t$ with respect to the initial position of the body at $t = 0$ is zero. The amplitude of precession is then given by $a'(\Delta t) = \theta_{XY}(\Delta t) + \beta$. This case is shown in Fig. 2 for $N = 2$ and inertia ratio $A/C = 10$.

2) If N_λ is an integer, then $a' = 0$, i.e., there is no precession at $t \geq \Delta t$. The body remains in a state of pure spin about the z axis tilted at an angle β with respect to the axis of symmetry 3, which describes a circle of a radius β. The angular position of z axis in space remains fixed and is given by $c' = \theta_{XY}(\Delta t) + \beta e^{in\cdot\Delta t}$ or by $c' = c^*(i/2\pi N)(1 - e^{i2\pi N})$ from Eq. (21). This case is shown in Fig. 3 for $N_\lambda = -2$ and $A/C = 10$. Note that scales of Figs. 2 and 3 are based on the same β (i.e., on the same slope of M). As a result, the final values of β differ in the ratio $(A - C)/A$. Heavy lines indicate motions at $t \leq \Delta t$; lighter lines indicate motions at $t \geq \Delta t$. Precessional paths are shown in dotted lines.

3) If $N = A/C$, where the inertia ratio A/C is an integer, then $N_\lambda = (1 - A/C)N$ is also in integer, and therefore $a' = c' = 0$, i.e., the final motion is one of pure spin about the z axis aligned with the inertial axis Z. The axis of symmetry of the body will describe a circle radius β centered on z.

4) As $N \to \infty$, $a' \to 0$, $c' \to 0$. The final motion is the same as in the preceding case.

Equation (22) is plotted in the X-Y plane in Fig. 4; since $a^* = |a^*|$ this plot represents the locus of $a'(\Delta t)$ at a constant

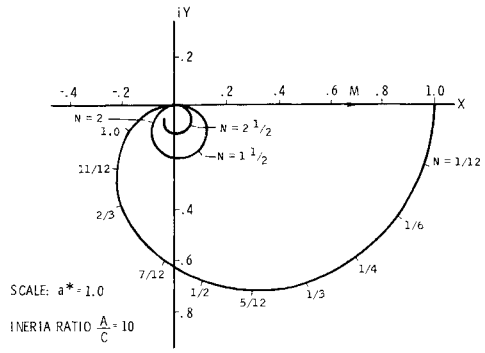

Fig. 4 Locus of the amplitude vector a' (Δt).

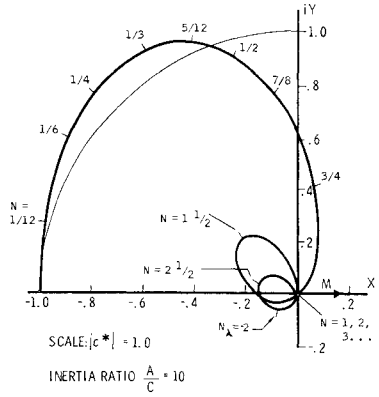

Fig. 6 Locus of the final center of motion, c'.

inertia ratio $A/C = 10$. The absolute value of the a'/a^* ratio as a function of N is plotted in Fig. 5. Evidently $|a'| < |a^*|$ always and the ratio $|a'/a^*|$ is a harmonic decaying function of relative spin revolutions N_λ. By differentiating Eq. (22), we readily establish that peaks of that function occur whenever $\tan \pi N_\lambda = \pi N_\lambda$.

Figure 6 presents the plot of the locus of $c'(\Delta t)$ in the form of $c'/|c^*|$ ratio again at constant $A/C = 10$. The ratio $|c'/c^*|$ is plotted in Fig. 7. It can be seen that $|c'|$ is smaller than $|c^*|$ and diminishes rapidly with an increase of N provided that $N > 0.45$ approx., i.e., provided that the body rotated through more than 165° during linear increase of the moment M. At all values of $N < 0.45$, the final mean attitude displacement under ramp input moment is greater than that under the step input, with $c'_{\max} = 1.1c^*$ occurring when $N = 0.29$. It is intuitively apparent that $|c'/c^*|_{\max}$ depends upon inertia ratio A/C and can only occur if $N < 0.5$. This becomes more evident upon expanding factored terms in Eq. (21), writing it in the form

$$c'/c^* = -(i/2\pi N)\cdot(n^2/\lambda^2)\{[(n^2 - \lambda^2)/n^2] \times (1 - e^{i2\pi N}) - e^{i2\pi N_\lambda} + e^{i2\pi(N+N_\lambda)}\} \quad (23)$$

which lends itself well to geometrical interpretation. However, purely analytical examination of Eq. (23) for $|c'/c^*|_{\max}$ at different inertia ratios is still impractical since (c'/c^*) is a multiple term transcendental function. To overcome this difficulty, Eq. (23) is expressed as

$$c'/c^* = -i(K/2\pi N)(E + iF)$$

where

$$K = n^2/\lambda^2$$

$$E = k(1 - 2\pi N) - \cos 2\pi N_\lambda + \cos 2\pi(N_\lambda + N)$$

$$F = -k \sin 2\pi N - \sin 2\pi N + \sin 2\pi(N_\lambda + N)$$

where

$$k = (n^2 - \lambda^2)/n^2$$

so that the magnitude of c'/c^* becomes

$$|c'/c^*| = (K/2\pi N)(E^2 + F^2)^{1/2}$$

Upon some manipulation, this reduces to

$$|c'/c^*| = [K/(2\pi N)^{1/2}]\{(k^2 - 2k \cos 2\pi N_\lambda + 1) \times (1 - \cos 2\pi N)\}^{1/2} \quad (24)$$

where

$$K = [R/(1 - R)]^2, \quad k = (2R - 1)/R^2, \quad \text{and} \quad N_\lambda = [(1 - R)/R]N$$

with R denoting the inertia ratio A/C.

Equation (24) lends itself readily to determination of maximum magnitude of c'/c^* at various inertia ratios R, and determination of N for $|c/c^*| = 1$ by application of a numerical differential correction procedure based upon Newton's root-seeking scheme,[6] with the use of the REACTS computing machine.

Figure 8 presents the results for the range of inertia ratios $3 \leqslant R \leqslant 20$. The top curve represents the maximum magnitude ratio c'/c^* as a function of A/C, while the bottom curve gives the corresponding N necessary for maximum displacement of the final center of motion. The middle curve represents the plot of values of N at which for a given inertia ratio the final displacement of the center of motion under ramp input moment is equal in magnitude to that under step input. Any point under that curve represents a combination of N and A/C values resulting in $|c'| > |c^*|$. In the region above that curve, $|c'| < |c^*|$ always. For example, if the inertia ratio of the rocket at ignition is, say, 4.5 and its spin rate is 60 rpm, then unless the time interval during which the moment increases linearly is $\Delta t \geq 0.62$ sec, the final mean attitude error may exceed that calculated under an assumption of a step input. If $\Delta t = 0.37$, $|c'|$ may exceed $|c^*|$ by 44% (max).

At lower inertia ratios, the excess of $|c'|$ over $|c^*|$ increases rapidly and the range of N at which such an excess is possible also increases. As inertia ratio approaches 2, $|c'/c^*|$ may ex-

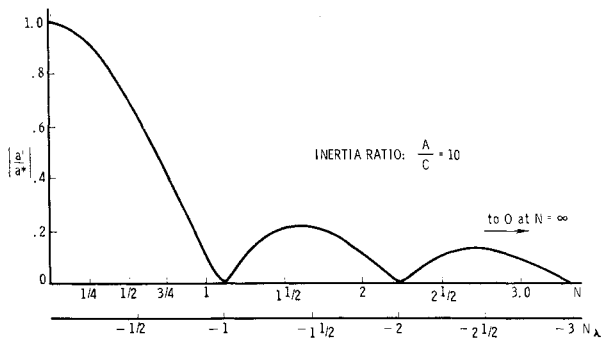

Fig. 5 Ratio $|a'/a^*|$ as a function of N.

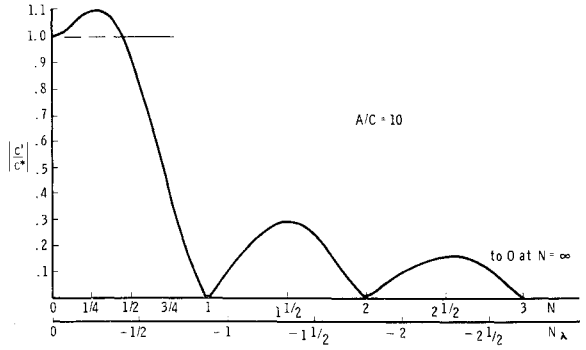

Fig. 7 Ratio $|c'/c^*|$ as a function of N.

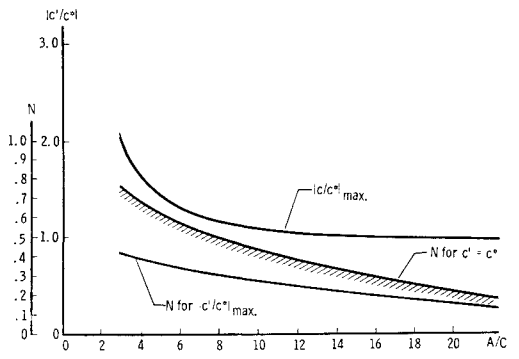

Fig. 8 Boundaries of $|c'/c^*|$ under ramp input.

ceed 1 during its second peak, i.e., at $N > 1.0$. This can be seen from the three-dimensional response surface of $|c'/c^*| = f(N,R)$ in Fig. 9, restricted in the interests of clarity to inertia ratios $2 \leqslant R \leqslant 15$.

Primary Conclusions and Discussion

Figures 4–9 provide a complete and detailed answer to the problem under consideration. Stated briefly, it is as follows. As the result of application of a body-fixed moment as a ramp input,

1) the amplitude of the coning motion is always decreased,

2) the average attitude displacement of a rocket will be increased if the slope of $M(t)$ is sufficiently high (and this is quite likely to occur in practice) for a given inertia ratio A/C and spin rate n; otherwise it will be decreased,

3) both $|a'/a^*|$ and $|c'/c^*|$ ratios are decaying harmonic functions of spin revolutions completed during the time interval when moment is increasing; thus both the final, steady-state coning angle and the displacement of the center of motion can be zero, either individually or together.

The analysis was carried out under the assumption $\omega_{12}(0) = \theta_{XY}(0) = 0$, which also implies $\varphi(0) = 0$. Inclusion of $\omega_{12}(0) \neq 0$ in the basic model would result in the presence of additional vectorially additive linear terms $\omega_{12}(0) \cdot e^{i\lambda t}$ and $i[\omega_{12}(0)/(n + \lambda)]\{1 - e^{i(\lambda+n)t}\}$ in all solutions for ω_{12} and θ_{XY}, respectively, both for a ramp input and a step input alike. To account for $\omega_{12}(0) \neq 0$ is a trivial task; however, its inclusion in the basic model would not only needlessly complicate the subsequent discussion but would also tend to obscure the subject under investigation. Inclusion of $\theta_{XY}(0) \neq 0$ would amount to adding a constant which could have no effect upon validity of the results within constraint $\cos\theta = 1$, $\sin\theta = \theta$. In practical applications, should $\theta_{XY}(0)$ be large (as it may become with a multistage rocket) one can easily get rid of its effect upon the accuracy of results by changing the orientation of the inertial axes by a desired amount. As for $\varphi(0)$, it is of no explicit concern at any time, because within the assumption of small θ it imposes no restriction upon validity of transformation formula $\theta_{XY} = \omega_{12}(0)e^{int}$. This is so because writing $\dot{\psi} + \dot{\varphi} = n$ (Ref. 4) implies that any axis in the transverse principal plane can be treated as a node axis, as far as transformation of angular velocity along that axis to any other axis is concerned.

Extensions and Applications

Results of the analysis lend themselves to further extensions and applications.

Interpretation of Rocket Attitude Patterns

It will be recalled that when the body-fixed moment and inertias remain constant [Eqs. (11, 14, 19, and 20)], the spin takes place about the axis z, which is inclinded to the axis of symmetry at an angle $\beta = -M/(C - A)n^2$, and describes a pure conical path; consequently, the axis of symmetry 3 traces nutations in the inertial space of constant amplitude β. It follows, therefore, that if nutations are cuspidal[1] the magnitude of the total cross-spin velocity vector ω_{xy} is greater or equal to $|\beta n|$; if it is less, nutations must be in the form of loops. In the special case of the two being equal, nutations are just cuspidal and tangents at each end of any cusp will pass through the center of precession. In another special case, $\omega_{12}(0) = -i\beta n$, $\omega_{xy} = 0$ at all times; there is no precession and nutations transform into circles. It is fairly obvious from purely geometrical considerations (for the sake of brevity we shall refrain from providing mathematical derivations)

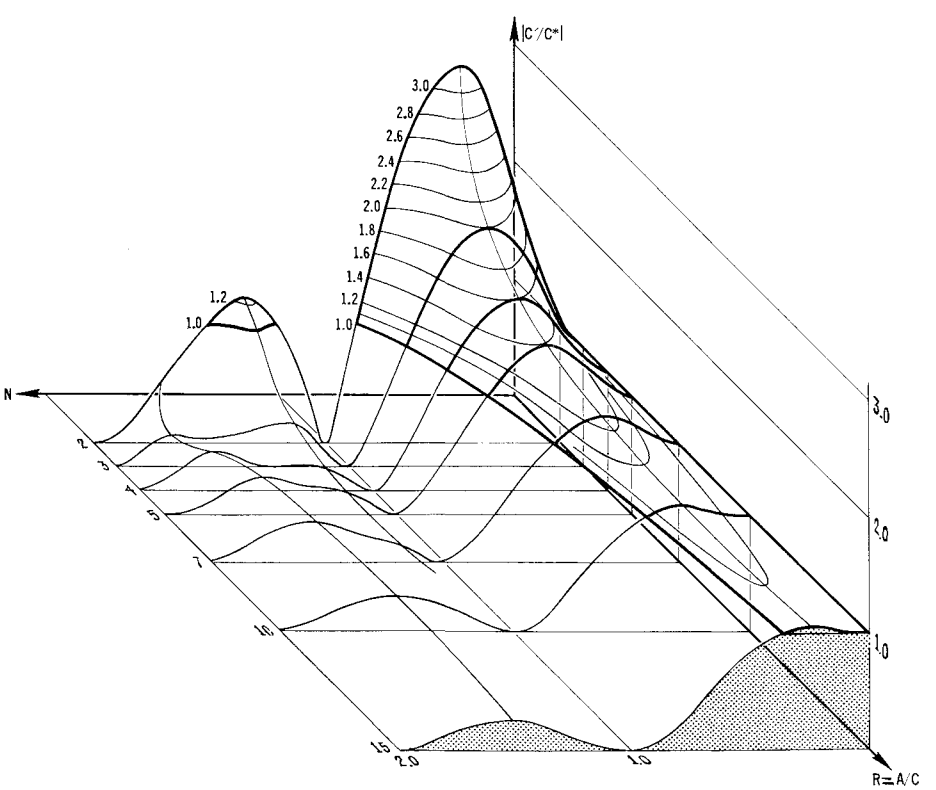

Fig. 9 Attitude error due to ramp input as a surface $f(|c'/c^*|,N,R)$.

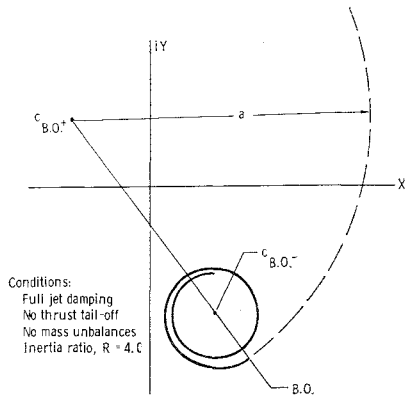

Fig. 10 Angular motions of a rocket before and after burnout.

that when β is constant an accurate trace of one complete nutation cycle in the X-Y plane provides enough data from which the coning angle, inertia ratio, position of the center of precession, and initial angular rate $\omega_{12}(0)$ can be determined. Similarly "residual motion" subsequent to rectangular input[2] can be readily determined from the body attitude at the input termination by either analytical or graphical means, provided that nutations are clearly shown on the plot of body attitude in space.

When the body-fixed moment increases linearly [Eqs. (13) and (17)], the magnitude of the cross-spin $\dot{\beta}n/\lambda$, thus formed, the amplitude of precession a, and the center of motion c all remain constant; but the position of the spin axis within the body varies with respect to the axis of symmetry 3 at the rate $\dot{\beta}$. As the result the amplitude of nutations traced by the axis of symmetry is increasing. The "growing loop characteristics" associated with variable inertia and variable moment case[1] reflect an increase in angle β and, to a lesser extent, decrease in the coning angle due to usual decrease of inertia ratio A/C during burning.

Thrusting Phase Phenomena

Upon reflection the results obtained in the course of the present analysis lead to a number of quite general observations, as follows. The cross-spin (and hence the coning angle) is neither produced nor changed by a mere presence of external body fixed moment; rather, it is produced or changed by instantaneous (or nearly so) changes in β and/or $\dot{\beta}$. Also, from the standpoint of the effect upon the cross-spin it is quite immaterial whether changes in β (or $\dot{\beta}$) are produced by variable moment or variable inertia. The center of motion similarly is virtually insensitive to gradual changes in the applied body fixed moment or in the inertia ratio. The amplitude and the rate of precession however, being governed directly by inertial (gyroscopic) effects, are sensitive to any changes in inertia ratio, sudden or gradual.

In a typical solid fuel space rocket with a burning time of 30–40 sec, the angle β may increase at an exponential rate up to 5 to 10 times of its initial (ignition) value. However, this change takes place without discontinuities; changes in inertia ratio are also continuous. Under these circumstances the center of motion will remain constant even though the center of precession may be describing small spiraling out, nearly circular paths. Jet damping cannot have any significant effect upon the center of motion because geometry of any real life rocket assures that jet damping moment must always be small with relation to disturbances responsible for cross-spin or transverse angular rate necessary for the very existance of jet damping moment. We may conclude therefore that variable moment and inertia resulting from mass transfer during burning, and jet damping, can have only very small second-order effects upon the average attitude during burning; for most practical purposes this attitude is fully determined by the initial conditions at ignition: $\theta_{XY}(0)$, $\omega_{12}(0)$, $\dot{M}(0)$, $M(0)$ and $C(0)$.

Burn-Out Phenomena

The results of the present analysis indicate also that the most obvious and primary reason for a sudden resumption or increase of coning motion at burn-out[7] is sudden removal of the body fixed moment due to thrust. This does not rule out other possible reasons for increase of coning at burn-out, such as fragments thrown from the rocket, thrust misalignment of the dying flame, or even deformation of the hot rocket, presented in Ref. 7 and often mentioned elsewhere. All of these, however, are highly conjectural, with the last one plainly inadmissible unless it be assumed that actual deformation occurs suddenly. On the other hand, existence of thrust misalignment of reasonably constant magnitude and direction can be taken for granted; often it can also be confirmed or even evaluated from the drop of the spin rate at ignition, observed in experimental data.[7] In this connection it is of interest to reflect upon the role of jet damping and thrust "tail off" at burn-out. In absence of jet damping, the amplitude of coning motion at burn-out could increase, decrease or even remain unchanged in magnitude depending upon the phase relationship between existing cross-spin vector and $\Delta\beta$ at burn-out. By suppressing initial wobble jet damping makes it certain that thrust termination will result in a substantial new cross spin rate about the new axis, together with attendant coning motion about the new center as shown in Fig. 10. Jet damping in spin, if present, will result in further increase of angle β during burning, which, however, will have no appreciable effect upon the center of motion until burn-out; but both the coning angle and the attitude displacement due to thrust termination will be thereby increased. The presence of thrust tailoff will tend to reduce sharply the magnitude of the coning angle subsequent to burnout and will affect the center of motion in a manner consistent with the change in β as formerly discussed. Evidently, if angular motions and attitude of payload are of interest, a complete thrusting phase solution, with variable moment, variable inertia and jet damping taken into account, is desirable.

Closing Comments

A distinct problem of practical interest and to the best of the author's knowledge not formerly analyzed has been subjected to a fully parameterized analysis, utilizing a complex variable technique and the notation of Ref. 4, both having been found exceptionally well suited for the task. A complete set of answers to the problem under consideration has been provided. Results were also extended to meaningful interpretation of thrusting phase and burn-out phenomena. Special emphasis was placed upon interpretation of angular motions in body coordinates, since these provide the key to understanding of body attitude plots in inertial space.

In spite of their simplicity and wide applicability the analytical solutions presented herein are exact within the usual small angle approximation; as such they require no comparisons with numerical machine solutions of nonlinearized equations of motion. Geometrical interpretation of angular motions along the lines developed in the present work is particularly useful in diagnostic analysis where the success of the investigation hinges upon proper recognition of angular motion traces obtained from experiment or simulation. The author is inclined to think that a similar approach, if applied to the recently much discussed problem of roll resonance (in connection with ballistic re-entry vehicles), would lead to a clear-cut and straightforward presentation of some of the main features of that problem.

References

[1] Jarmolow, K., "Dynamics of a Spinning Rocket with Varying Inertia and Applied Moment," *Journal of Applied Physics*, Vol. 28, 1957, pp. 308–313.

[2] Suddath, J. H., "A Theoretical Study of the Angular Motions of Spinning Bodies in Space," Rept. 83, 1961, NASA.
[3] Buglia, J. J. et al., "Analytical Method of Approximating the Motion of a Spinning Vehicle with Variable Mass and Inertia Properties Acted Upon by Several Disturbing Parameters," Rept. 110, 1961, NASA.
[4] Thompson, W. T., *Introduction to Space Dynamics*, Wiley, New York, 1961.
[5] Rausher, M., *Introduction to Aeronautical Dynamics*, Wiley, New York, 1953.
[6] Junkins, J. L., "Astrodynamics Training Course Documentation," Rept. MDAC-61705, Sept. 1968, McDonnell-Douglas Corp., Santa Monica, Calif.
[7] Mott, D. L., "The Rotation of Syncom III During Launch," X-621-64-294, Oct. 1964, Goddard Space Flight Center, Greenbelt, Md.

MARCH 1970 J. SPACECRAFT VOL. 7, NO. 3

Application of a Colored Noise Kalman Filter to a Radio-Guided Ascent Mission

DONALD J. JOHNSON*
The Aerospace Corporation, El Segundo, Calif.

A set of general sequential filter equations is derived for nonlinear system dynamics and a nonlinear observation model, but is obtained with the assumption of a linear estimator. These equations, which are based upon previously developed formulas, include the colored measurement noise statistics and the statistics of nonestimated model parameter errors. Several simulations made with this filter are compared with the simulation results of an estimation procedure constructed with the utilization of the standard white noise assumptions. The difference between the white noise filter results and the colored noise filter results is found to be minimal. Instability occurred when the statistics of the effective exhaust velocity in the acceleration model were not properly accounted for.

Nomenclature

A = $\left.\frac{\partial h}{\partial T}\right|_{\substack{X=\hat{X}_{n/n-1}\\T=\hat{T}}} - \rho\left.\frac{\partial h}{\partial T}\right|_{\substack{X=\hat{X}_{n/n-1}\\T=\hat{T}}}$
B $\equiv E[\delta\hat{T}\delta\hat{T}^T]$
D = $\left.\frac{\partial \phi}{\partial p}\right|_{\substack{X=\hat{X}_{n/n-1}\\p=\hat{p}}}$
E = the expectation operator
H_a = $H_n\Phi - \rho H_{n-1}$
H_n = $\left.\frac{\partial h}{\partial X}\right|_{\substack{X=\hat{X}_{n/n-1}\\T=\hat{T}}}$
K_n = the filter gain matrix
L_n $\equiv E[\delta\hat{X}_{n/n}\delta\hat{T}^T]$
n = subscript associating variable with the nth time point
$n/n-1$ = subscript indicating that the variable is evaluated at the nth time point and is based upon measurements up to and including the $(n-1)$st
N_n = vector of measurement noise
p = dynamic model parameter vector
$\hat{p}$ = an estimate of p; $\delta\hat{p} = p - \hat{p}$
Q,R,S $\equiv E[\mu_n\mu_n^T]$, $E[W_nW_n^T]$, and $E[\delta\hat{p}\,\hat{p}^T]$, respectively
T = measurement model parameter vector
$\hat{T}$ = an estimate of T; $\delta\hat{T} = T - \hat{T}$
V_n = $E[\delta\hat{X}_{n/n}\delta\hat{p}^T]$
W_n = a white noise vector
X_n = the state vector
$\hat{X}_{n/i}$ = the estimate of the state vector at t_n given all measurements up to and including that at t_i
z_n = the measurement vector
ζ_n = effective measurement after differencing
$\hat{\zeta}_n$ = estimated effective measurement computed from $\hat{X}_{n/n-1}$
μ_n = white process noise vector
Γ,Φ = $\left.\frac{\partial \phi}{\partial \mu}\right|_{\substack{X=\hat{X}_{n/n-1}\\p=\hat{p}}}$ and $\left.\frac{\partial \phi}{\partial X}\right|_{\substack{X=\hat{X}_{n/n-1}\\p=\hat{p}}}$, respectively
ρ = correlation coefficient matrix representing the correlation between N_n and N_{n-1}

Received August 14, 1969; presented as Paper 69-840 at the AIAA Guidance, Control, and Flight Mechanics Conference, Princeton, New Jersey, August 18–20, 1969; revision received December 18, 1969.

* Member of the Technical Staff, Space Guidance Section, Guidance and Analysis Dept. Member AIAA.

Introduction

DURING radio-guided launch missions (Fig. 1), angle measurement noise is more bothersome at low radar line-of-sight elevation angles. Significantly, a greater portion of the launch guidance occurs at low-elevation angles when larger boost vehicles are used. Random fluctuations in the tropospheric index of refraction are slower and more severe in the low-altitude regions and thus affect not only the magnitude but also the autocorrelation of the angle errors

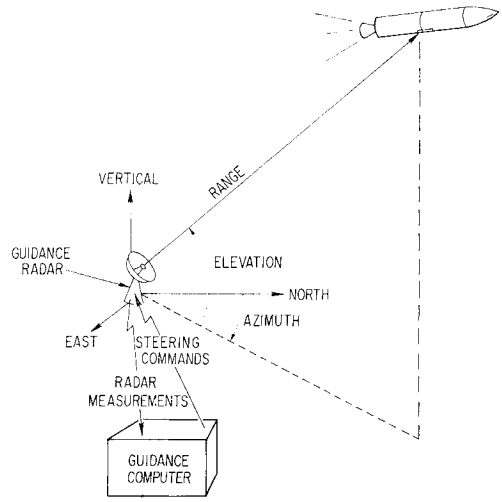

Fig. 1 Launch guidance radar system.